Journal of Harbin Engineering University
ISSN: 1006-7043
Vol 44 No. 9
September 2023

Motion Deblurring by Solving a New Optimization Problem

Meysam Gorji[1] Ali Tavakoli
Mathematics department, University of Mazandaran, Babolsar, Iran
[1] Corresponding author: m.gorji05@umail.umz.ac.ir

Abstract- The Wiener filter is effective in restoring degraded images caused by linear motion blur when the parameters of the blur are known. This paper presents an optimization problem to estimate the appropriate parameters of the motion blur. To solve this problem, a particle swarm optimization algorithm is employed. Extensive experiments conducted on the GoPro dataset demonstrate the superiority of the proposed framework compared to other state-of-the-art techniques for image motion deblurring.

Keywords- Motion deblurring; Wiener filter; particle swarm optimization.

1. Introduction

One of the common problems in image processing is the blurring of images, which occurs when it is difficult to distinguish the details of the image. A blurred image is also referred to as a degraded image. In restoration, similar to image enhancement techniques, we seek to improve the image; however, image recovery methods first determine the degradation model and then restore the original image in a reverse process. The necessity of deblurring images in medical, personal, astronomical, microscopic, military, etc. contexts cannot be denied. Deblurring is very difficult because it is possible that the blurring changes in different parts of the image. Even if it is the same throughout the image, the blurring is still an ill-posed problem. Deblurring operations are divided into non-blind, blind, and semi-blind, depending on whether the blurred kernel is known or unknown [1-2]. Non-blind deblurring strategies restore blurred images by predicting the inverse process using the known blurred kernel. The classical techniques use the Wiener filter, LR (Lucy–Richardson), and Kalman filter techniques [9]. Non-blind methods have been proposed in works such as [4] and [6], where they solve this problem by using prior information about the image in a Bayesian or Maximum a Posteriori (MAP) framework. Often, blind deblurring algorithms use an iterative process that periodically estimates the kernel and the final image. During this process, the final image is obtained from the kernel and the blurred image by performing non-blind deblurring. This improved estimate from the image is then used to estimate the kernel in the next iteration. In [17], an iterative algorithm was used for blind deblurring.

Motion blurring prevalent type of is a blurring and a key cause of decreased image quality. Camera shaking or fast-moving objects and shorter exposure times can cause motion blurring when capturing images, affecting the transmission of image information and resulting in poor image perception [3,5].

In [14], Levin presented a blind motion deblurring method for images blurred due to camera shake. In [16], a fast motion deblurring technique was presented that reduced the computational operations for kernel estimation and sharpening. To estimate the kernel, the optimization function was modeled using image derivatives, and the number of processes was reduced by reducing the number of Fourier transformations required for the conjugate gradient method. Although Cho's algorithm is relatively fast, its performance is slightly weaker than that of previous works. Shi et al. [9] proposed a fast-deblurring strategy to focus on linear motion blur for 2D barcodes, using a line-search approach to effectively achieve the deblurred image. Zhang et al. [7] proposed the Deblur-GAN method for blind motion deblurring, which utilizes conditional generative adversarial networks (GANs) to improve the accuracy and visual quality of the deblurred results. In [10], Zheng presented a real-time object detection algorithm that incorporates blind motion deblurring to improve the accuracy of object detection in blurry images.

The proposed algorithms have led to enhancements in classical methods such as the Wiener filter, emphasizing the need for an efficient algorithm to effectively restore images affected by motion blur. The objective of this paper is to utilize a novel optimization algorithm for the blind deblurring of linear motion blurred images. Through experimental results, we demonstrate the effectiveness of our proposed method in accurately estimating the parameters associated with motion blur. This paper is organized as follows:

Section 2.1 explains the motion-blurred images. Section 2.2 discusses deblurring via the Wiener filter. Section 3 describes the proposed optimization problem for linear motion deblurring and employs the particle swarm optimization algorithm to adjust parameters in the problem. The experiments and concluding remarks are in Sections 4 and 5, respectively.

2. Materials and Methods

2.1. Motion blurred images

In this section, we explain how a motion blurred image appears. In general, it can be described by a discrete Fourier transform and its inverse, which we define in the sequel.

Definition 1. (2-D Discrete Fourier Transform and Its Inverse)

Let M and N be two integer numbers. The 2-D discrete Fourier transform of a function $f: \{0,1,2,\dots M-1\} \times \{0,1,2,\dots N-1\} \to \mathbb{R}$, denoted by $F: \{0,1,2,\dots M-1\} \times \{0,1,2,\dots N-1\} \to \mathbb{R}$, is defined as follows:

$$F(u,v) = \sum_{x=0}^{M-1} \sum_{y=0}^{N-1} f(x,y)\ e^{-j2\pi\left(\frac{ux}{M}+\frac{vy}{N}\right)}, \quad (1)$$

$u = 0,1,\dots,M-1$, $v = 0,1,\dots,N-1$.

Also, the inverse discrete Fourier transform of a function $F(u,v)$ is define by:

$$f(x,y) = \frac{1}{MN} \sum_{u=0}^{M-1} \sum_{v=0}^{N-1} F(u,v)\ e^{j2\pi\left(\frac{ux}{M}+\frac{vy}{N}\right)}, \quad (2)$$

$x = 0,1,\dots,M-1,\ y = 0,1,\dots,M-1.$

The blurred image caused by motion can be created by convolution of a Point Spread Function (PSF) $p(x,y)$ and the original image $f(x,y)$ with the addition of noise $n(x,y)$, i.e., [10-11].

$$g(x,y) = p(x,y) * f(x,y) + n(x,y). \quad (3)$$

The function $p(x,y)$ is a filter that convolves on the original image. It affects the neighboring pixels of an original pixel and blurs the pixel.

For example, an *average filter* blurs the original image. The Fourier transform of (3) gives:

$$G(u,\mathrm{v}) = P(u,v)F(u,v) + N(u,v). \quad (4)$$

Suppose the image $f(x,y)$ is blurred by a uniform linear motion with the values of $x_0(t)$ and $y_0(t)$, which are respectively motion in the direction of x and y. if T is the duration of the exposure, the blurred image $g(x,y)$ is obtained as follows [12]:

$$g(x,y) = \int_0^T f\,[x - x_0(t), y - y_0(t)\ ]\,dt. \quad (5)$$

The Fourier transform of (5) is written as follows:

$$G(u,v) = \int_0^T \Big(\int_{-\infty}^{\infty}\int_{-\infty}^{\infty} f[x - x_0(t), y - y_0(t)]\ e^{-j2\pi(ux+vy)}\,dxdy\Big)\,\mathrm{dt}. \quad (6)$$

Using the properties of integration and the definition of Fourier transform, we will have the following equation:

$$G(u,v) = F(u,v)\int_0^T e^{-j2\pi(ux_0(t)+vy_0(t))}\ dt. \quad (7)$$

According to (4), the following equation holds:

$$P(u,v) = \int_0^T e^{-j2\pi(ux_0(t)+vy_0(t))}\ dt. \quad (8)$$

If the motion variables $x_0(t)$ and $y_0(t)$ are known, $P(u,v)$ can be obtained directly from (8).

Let a and b be unknown values, and h_0 and k_0 be given values. a and b are motion-blur parameters that determine the direction of motion blurring. Moreover, we assume that the image is blurred by uniform linear motion between the sensor and the scene at the time of imaging. For this sake, one can consider $x_0(t) = h_0 + \frac{at}{T}$ and $y_0(t) = k_0 + \frac{bt}{T}$. For simplicity, we consider $h_0 = k_0 = 0$. Now, the relation (8) is written as follows:

$$P(u,v) = \int_0^T e^{-j2\pi\left(\frac{uat}{T}+\frac{vbt}{T}\right)}\ dt \quad (9)$$
$$= \frac{-T}{j2\pi(ua+vb)} e^{-j\pi(ua+vb)}\left(-2j\sin\big(\pi(ua+vb)\big)\right).$$

$p(x,y)$ is obtained as follows:

$$P(u,v) = \frac{T}{\pi(ua+vb)}\ sin\,[\pi(ua+vb)]\,e^{-j\pi(ua+vb)}. \quad (10)$$

2.2. Deblurring via Wiener filter

The Wiener filter tries to find an approximation of the original image. The method is founded on considering images and noise as random variables, and the objective is to find an estimate $\hat{f}$ of the uncorrupted image f such that the mean square error between them is minimized. This error measure is given by $e = E\{(f-\hat{f})^2\}$, where $E\{.\}$ is the expected value of the argument. In the frequency domain, the restored image is obtained as follows:

$$\hat{F}(u,v) = R(u,v)G(u,v), \tag{11}$$

The Wiener filter is obtained as follows:

$$R(u,v) = \left[\frac{1}{P(u,v)}\frac{|P(u,v)|^2}{|P(u,v)|^2 + C}\right], \tag{12}$$

The terms in (12) are as follows: $P(u,v)$ is a degradation function, $|P(u,v)|^2 = P^*(u,v)P(u,v)$, $P^*(u,v)$ is the complex conjugate of $P(u,v)$, and $C = \frac{S_\eta(u,v)}{S_f(u,v)}$ is the ratio of noise power to signal power. As a result, $\hat{F}$ is obtained as follows:

$$\hat{F}(u,v) = \left[\frac{1}{P(u,v)}\frac{|P(u,v)|^2}{|P(u,v)|^2 + C}\right] G(u,v). \tag{13}$$

Now, the deblurred image $\hat{f}$ is obtained by inverse Fourier transform from (13).

3. Proposed method

As we said in Section 2, the values a and b determine the direction of motion blurring. When the values of a and b are known, the Wiener filter can deblur the motion-blurred image well. However, the exact values of a and b are usually unknown. In this section, we present a novel method for finding these values.

The image formed by the edges of a motion-blurred image usually has a large dispersion. In other words, for a motion-blurred image $g(x,y)$, the image created by the absolute gradient of $g(x,y)$ has usually a large variance, whereas this is not usually the case in the original image. Therefore, our aim is to minimize the variance of the absolute gradient of the deblurred image. To this end, let $\hat{f}(x,y)$ be the deblurred image by the Wiener filter with PSF parameters a, b. The proposed optimization problem for motion deblurring is given by:

$$\min_{a,b} \quad U(a,b) = var\left(\left|\nabla \hat{f}_{a,b}\right|\right), \tag{14}$$

where

$$\left|\nabla \hat{f}\right| = \sqrt{\left(\frac{\partial \hat{f}(x,y)}{\partial x}\right)^2 + \left(\frac{\partial \hat{f}(x,y)}{\partial y}\right)^2}, \tag{15}$$

denotes the absolute gradient of the deblurred image $\hat{f}(x,y)$.

Since the Problem (14) is non-convex, we use the heuristic method, Particle Swarm optimization (PSO), to find the global minimum (see Algorithm PSO).

Algorithm PSO

Step 1: Initialize position $\begin{bmatrix} a_i \\ b_i \end{bmatrix}$ and velocity $\begin{bmatrix} v_{a_i} \\ v_{b_i} \end{bmatrix}$ for each particle i.

Step 2: Evaluate the fitness function $U(a_i, b_i)$ for each particle i.

If the fitness value is better than the best fitness value ($gBest$), then set the new value as the new $gBest$ and choose the particle with the best fitness value as the $gBest$.

Step 3: For each particle, update the velocity and position as follows:

$$\begin{bmatrix} a_i^{t+1} \\ b_i^{t+1} \end{bmatrix} = \begin{bmatrix} a_i^t \\ b_i^t \end{bmatrix} + \begin{bmatrix} v_{a_i}^t \\ v_{b_i}^t \end{bmatrix}, \tag{16}$$

$$\begin{bmatrix} v_{a_i}^{t+1} \\ v_{b_i}^{t+1} \end{bmatrix} = w \begin{bmatrix} v_{a_i}^t \\ v_{b_i}^t \end{bmatrix} + s_1 r_1 \left(\begin{bmatrix} aBest_i^t \\ bBest_i^t \end{bmatrix} - \begin{bmatrix} a_i^t \\ b_i^t \end{bmatrix} \right) + s_2 r_2 \left(\begin{bmatrix} gBest_{a_i}^t \\ gBest_{b_i}^t \end{bmatrix} - \begin{bmatrix} a_i^t \\ b_i^t \end{bmatrix} \right), \tag{17}$$

where v_i^{t+1} is the velocity of particle i at the $(t+1)$-th iteration, w is the inertia weight, and $\begin{bmatrix} a_i^t \\ b_i^t \end{bmatrix}$ is the position of particle i in the t-th iteration. $\begin{bmatrix} gBest_{a_i}^t \\ gBest_{b_i}^t \end{bmatrix}$ implies the global best position of any particle in the t-th iteration. $\begin{bmatrix} aBest_i^t \\ bBest_i^t \end{bmatrix}$ indicates the personal best position of particle i in the t-th iteration. r_1 and r_2 stand for random numbers uniformly distributed in the range [0,1], and s_1 and s_2 represent the cognitive and social parameters [15,18].

Step 4: Evaluate the fitness function $U(a_i^t, b_i^t)$. Find the current best $\begin{bmatrix} gBest_{a_i} \\ gBest_{b_i} \end{bmatrix}$.

Step 5: Update $t := t + 1$. Output: $\begin{bmatrix} gBest_{a_i} \\ gBest_{b_i} \end{bmatrix}$ and $\begin{bmatrix} a_i^t \\ b_i^t \end{bmatrix}$.

4. Experiments

4.1 Evaluation measures and dataset

In this study, we utilized the widely employed GoPro dataset [19] for motion deblurring to train and evaluate models. The GoPro dataset consists of 3,214 pairs of sharp and blurry images with dimensions of 1280×720. To compare the motion deblurring performance of our framework with some baseline models (Multi-scale Network [19], Deblur-GAN [7], and Cross-modal Attention [8]), two criteria were used: Structural Similarity (SSIM) and Peak Signal to Noise Ratio (PSNR) (dB).

4.2 Experimental results and discussion

Our motion deblurring pipeline was implemented in Matlab 2021a, and the experiments were conducted on a system with a Core i7 Intel(R) processor, 8 GB RAM, 3.2GHz, and GTX 3050 Ti GPU. We evaluated the quantitative and qualitative performance of our method compared to three other models: Multi-scale

Network [19], Deblur-GAN [7], and Cross-modal Attention [8].

The proposed method was applied to Fig. 1 (B), and the result was obtained in 30 iterations within 5 seconds of CPU time. The SSIM and PSNR values obtained using our method and the baseline models are listed in Table 1. The highest SSIM and PSNR values for each measure in Table 1 are highlighted in bold. From Table 1, it is evident that our strategy achieved the highest SSIM and PSNR values. The Multi-scale Network [19] showed the worst results (PSNR = 29.80 and SSIM = 0.941), while our proposed technique demonstrated a significant improvement over all models (PSNR = 38.84 and SSIM = 0.978). Additionally, there is a slight difference in the SSIM and PSNR values obtained using Deblur-GAN [7] and Multi-scale Network [19] models. The SSIM and PSNR values indicate that Multi-scale Network [19] and Deblur-GAN [7] are not as effective as the proposed and Cross-modal Attention [8] models.

Table 1. The results of the assessment measures of the four motion deblurring models.

Methods	PNSR(dB)	SSIM
Deblur-GAN [7]	32.35	0.958
Multi-scale Network [19]	29.80	0.941
Cross-modal Attention [8]	36.46	0.962
Proposed	**32.84**	**0.978**

Figures 1 to 3 display the qualitative results of the GoPro dataset. Cross-modal Attention [8] effectively restores edges, but exhibits some noise issues. In contrast, our suggested strategy demonstrates superior motion deblurring performance in challenging scenarios such as low-light environments, outdoor camera shake, and outdoor object movement, as illustrated in Figures 1 to 3. Furthermore, the obtained results provide evidence that our framework minimizes object deformation and yields sharper edges compared to previous models.

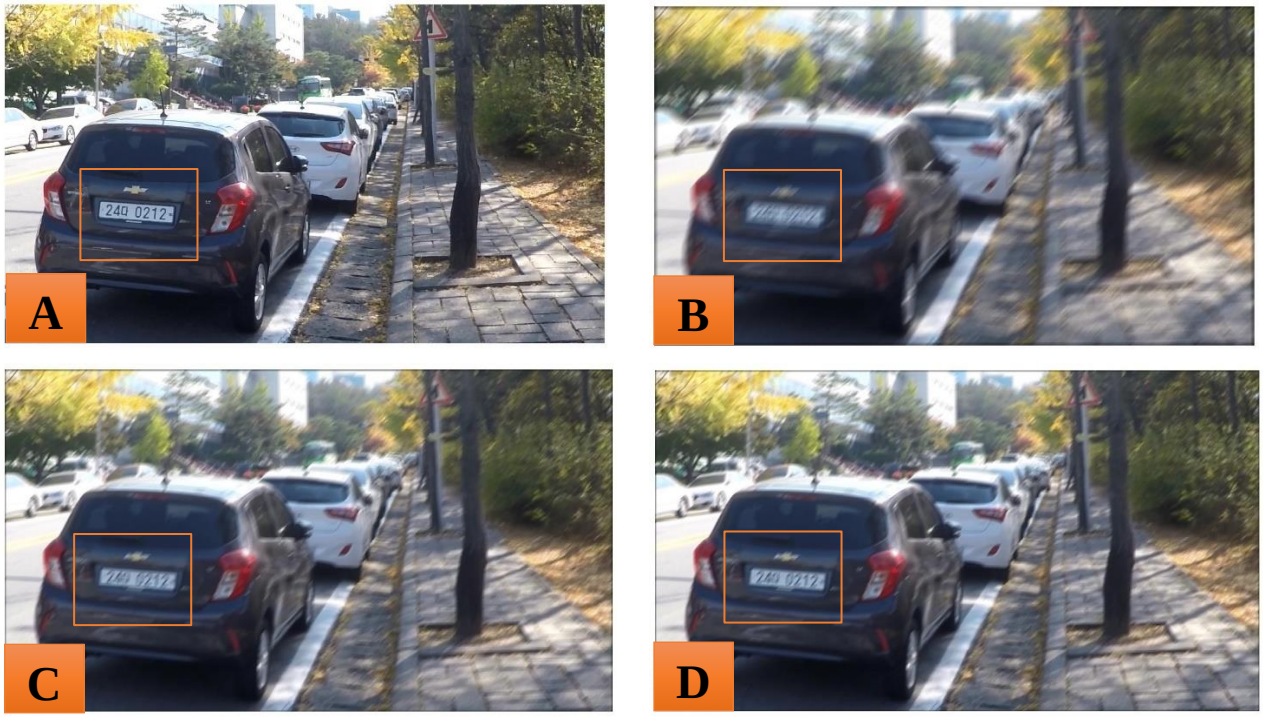

Fig. 1. Visual comparison of different deblurring models. A) original image, B) blurred image C) Multi-scale Network [19], D) Deblur-GAN [7], E) Cross-modal Attention [8], F) Ours.

Fig. 2. Visual comparison of different deblurring models. A) original image, B) blurred image C) Multi-scale Network [19], D) Deblur-GAN [7], E) Cross-modal Attention [8], F) Ours.

Fig. 3. Visual comparison of different deblurring models. A) original image, B) blurred image C) Multi-scale Network [19], D) Deblur-GAN [7], E) Cross-modal Attention [8], F) Ours.

5 Conclusion

In this paper, we stated an optimization problem to estimate motion blur parameters. The variance of the image edges was employed for this purpose. In the following, we solved this problem using the Particle Swarm Optimization (PSO) algorithm. However, when dealing with non-linear motion blur, it becomes necessary to redefine the optimization problem. The extensive experiments conducted on the GoPro dataset demonstrate that our framework yields high-quality images with distinct edge details.

References

[1] Belyaev, A. G., & Fayolle, P. A. (2022). Black-box image deblurring and defiltering. *Signal Processing: Image Communication*, *108*, 116833.

[2] Cohen, R., Elad, M., & Milanfar, P. (2021). Regularization by denoising via fixed-point projection (RED-PRO). *SIAM Journal on Imaging Sciences*, *14*(3), 1374-1406.

[3] Nair, N. G., Yasarla, R., & Patel, V. M. (2022, October). NBD-GAP: Non-Blind Image Deblurring without Clean Target Images. In *2022 IEEE International Conference on Image Processing (ICIP)* (pp. 3431-3435). IEEE.

[4] Gong, M., Jiang, X., & Li, H. (2017). Optimization methods for regularization-based ill-posed problems: a survey and a multi-objective framework. *Frontiers of Computer Science*, *11*(3), 362-391.

[5] Zhang, Y., Ma, S. Y., Zhang, X., Li, L., Ip, W. H., & Yung, K. L. (2020). EDGAN: motion deblurring algorithm based on enhanced generative adversarial networks. *The Journal of Supercomputing*, *76*(11), 8922-8937.

[6] Welk, M. (2016). A robust variational model for positive image deconvolution. *Signal, Image and Video Processing*, *10*(2), 369-378.

[7] Shao, W. Z., Liu, Y. Y., Ye, L. Y., Wang, L. Q., Ge, Q., Bao, B. K., & Li, H. B. (2020). DeblurGAN+: Revisiting blind motion deblurring using conditional adversarial networks. *Signal Processing*, *168*, 107338.

[8] Sun, L., Sakaridis, C., Liang, J., Jiang, Q., Yang, K., Sun, P., ... & Gool, L. V. (2022, November). Event-based fusion for motion deblurring with cross-modal attention. In *Computer Vision–ECCV 2022: 17th European Conference, October 23–27, 2022, Proceedings, Part XVIII* (pp. 412-428). Cham: Springer Nature Switzerland.

[9] Shi, Y., He, B., Zhu, M., & Zhang, L. (2020). Fast linear motion deblurring for 2D barcode. *Optik*, *219*, 164902.

[10] Zheng, S., Wu, Y., Jiang, S., Lu, C., & Gupta, G. (2021, July). Deblur-yolo: Real-time object detection with efficient blind motion deblurring. In *2021 International Joint Conference on Neural Networks (IJCNN)* (pp. 1-8). IEEE.

[11] Zhang, J., Zhang, C., Wang, J., Xiong, Q., Zhang, Y., & Zhang, W. (2021, July). Attention driven self-similarity capture for motion deblurring. In *2021 IEEE International Conference on Multimedia and Expo (ICME)* (pp. 1-6). IEEE.

[12] Gonzalez, Rafael C., and Woods, Richard E. Digital Image Processing. 4th ed., Pearson Education, 2018.

[13] Tavakoli, A., Mousavi, P., & Zarmehi, F. (2018). Modified algorithms for image inpainting in Fourier transform domain. *Computational and Applied Mathematics*, *37*(4), 5239-5252.

[14] Levin, A. (2006). Blind motion deblurring using image statistics. *Advances in Neural Information Processing Systems*, *19*.

[15] Jain, M., Saihjpal, V., Singh, N., & Singh, S. B. (2022). An Overview of Variants and Advancements of PSO Algorithm. *Applied Sciences*, *12*(17), 8392.

[16] Cho, S., & Lee, S. (2009). Fast motion deblurring. In *ACM SIGGRAPH Asia 2009 papers* (pp. 1-8).

[17] Yang, H., Su, X., & Chen, S. (2020). Blind image deconvolution algorithm based on sparse optimization with an adaptive blur kernel estimation. *Applied Sciences*, *10*(7), 2437.

[18] Tharwat, A., & Schenck, W. (2021). A conceptual and practical comparison of PSO-style optimization algorithms. *Expert Systems with Applications*, *167*, 114430.

[19] Nah, S., Hyun Kim, T., & Mu Lee, K. (2017). Deep multi-scale convolutional neural network for dynamic scene deblurring. In *Proceedings of the IEEE conference on computer vision and pattern recognition* (pp. 3883-3891).

[20] Cai, J., Wei, H., Yang, H., & Zhao, X. (2020). A novel clustering algorithm based on DPC and PSO. *IEEE Access*, *8*, 88200-88214.

[21] Chen, L., Fang, F., Wang, T., & Zhang, G. (2019). Blind image deblurring with local maximum gradient prior. In *Proceedings of the IEEE/CVF Conference on Computer Vision and Pattern Recognition* (pp. 1742-1750).

[22] Shen, Z., Wang, W., Lu, X., Shen, J., Ling, H., Xu, T., & Shao, L. (2019). Human-aware motion deblurring. In *Proceedings of the IEEE/CVF International Conference on Computer Vision* (pp. 5572-5581).

[23] Honarvar Shakibaei Asli, B., Zhao, Y., & Erkoyuncu, J. A. (2021). Motion blur invariant for estimating motion parameters of medical ultrasound images. *Scientific Reports*, *11*(1), 1-13.

[24] Yang, H., Su, X., & Chen, S. (2020). Blind image deconvolution algorithm based on sparse optimization with an adaptive blur kernel estimation. *Applied Sciences*, *10*(7), 2437.

[25] Cho, S., Cho, H., Tai, Y. W., & Lee, S. (2012, September). Registration Based Non-uniform Motion Deblurring. In *Computer Graphics Forum* (Vol. 31, No. 7, pp. 2183-2192). Oxford, UK: Blackwell Publishing Ltd.

[26] Chakrabarti, A. (2016). A neural approach to blind motion deblurring. In *Computer Vision–ECCV 2016: 14th European Conference, Amsterdam, The Netherlands, October 11-14, 2016, Proceedings, Part III 14* (pp. 221-235). Springer International Publishing.

[27] Xu, F., Yu, L., Wang, B., Yang, W., Xia, G. S., Jia, X., ... & Liu, J. (2021). Motion deblurring with real events. In *Proceedings of the IEEE/CVF International Conference on Computer Vision* (pp. 2583-2592).